

# Reversible acetylation of the chromatin remodelling complex NoRC is required for non-coding RNA-dependent silencing

Yonggang Zhou<sup>1,3</sup>, Kerstin-Maike Schmitz<sup>1,3</sup>, Christine Mayer<sup>1</sup>, Xuejun Yuan<sup>1</sup>, Asifa Akhtar<sup>2</sup> and Ingrid Grummt<sup>1,4</sup>

**The SNF2h (sucrose non-fermenting protein 2 homologue)-containing chromatin-remodelling complex NoRC silences a fraction of ribosomal RNA genes (rDNA) by establishing a heterochromatic structure at the rDNA promoter<sup>1-3</sup>. Here we show that the acetyltransferase MOF (males absent on the first) acetylates TIP5, the largest subunit of NoRC, at a single lysine residue, K633, adjacent to the TIP5 RNA-binding domain, and that the NAD<sup>+</sup>-dependent deacetylase SIRT1 (sirtuin-1) removes the acetyl group from K633. Acetylation regulates the interaction of NoRC with promoter-associated RNA (pRNA), which in turn affects heterochromatin formation, nucleosome positioning and rDNA silencing. Significantly, NoRC acetylation is responsive to the intracellular energy status and fluctuates during S phase. Activation of SIRT1 on glucose deprivation leads to deacetylation of K633, enhanced pRNA binding and an increase in heterochromatic histone marks. These results suggest a mechanism that links the epigenetic state of rDNA to cell metabolism and reveal another layer of epigenetic control that involves post-translational modification of a chromatin remodelling complex.**

Plasticity in transcription regulation can be achieved by dynamic regulation of the chromatin structure, involving ATP-dependent changes in nucleosome positions, modification of histone tails or DNA methylation. Acetylation of K16 on histone H4 (H4K16ac) is critical for chromatin decondensation, transcriptional activity and dosage compensation in *Drosophila melanogaster*<sup>4-7</sup>. Many transcriptional regulators, such as p300/CBP, GCN5 and MOF, have been proven to be histone acetyltransferases<sup>8,9</sup>. *Drosophila* MOF acetylates histone H4 (at K16) and other proteins, including MSL3, a subunit of the dosage compensation complex. Acetylation modulates the interaction of MSL3 with *roX2* RNA<sup>7,10,11</sup>.

Here, we present data showing that the activity of NoRC, which consists of TIP5 and SNF2h (ref. 1), is regulated by mammalian MOF- and SIRT1-dependent acetylation and deacetylation. NoRC mediates silencing of a

fraction of rDNA by recruiting histone-modifying enzymes and DNA methyltransferases, leading to heterochromatin formation and transcriptional silencing<sup>1-3,12</sup>. NoRC also shifts the promoter-bound nucleosome into a position that prevents transcription complex formation<sup>13</sup>. As binding of NoRC to rDNA requires the interaction of TIP5 with acetylated H4K16, which is acetylated by MOF<sup>14-17</sup>, we surmised that MOF might regulate the epigenetic state of rDNA. Indeed, chromatin immunoprecipitation (ChIP) experiments showed that MOF is associated with rDNA, the level of MOF and H4K16ac being higher at the promoter region than in the pre-rRNA coding region (Supplementary Information, Fig. S1a). Depletion of MOF decreased the association of H4K16ac and mouse TIP5 with rDNA and impaired nucleolar localization of NoRC (Supplementary Information, Fig. S1b, c). Digestion of immunoprecipitated DNA with the methylation-sensitive restriction enzyme *HpaII* revealed that DNA polymerase I (Pol I) was exclusively found at active, unmethylated rRNA genes, whereas mTIP5 and the heterochromatic trimethylated histone mark H4K20me3 were associated with methylated rDNA copies (Fig. 1a). In contrast, MOF and H4K16ac occupied both methylated and unmethylated rDNA copies, suggesting that they may have roles both in activating and silencing rRNA genes.

To examine whether MOF is involved in NoRC-dependent rDNA silencing, we assayed the interaction of MOF with TIP5 *in vivo* and *in vitro*. As shown in Fig. 1b, MOF but not Pol I co-precipitated with TIP5, at the region adjacent to its TAM (TIP5, ARBP and MBD) domain, required for MOF binding (Supplementary Information, Fig. S2a). In an *in vitro* assay with radiolabelled acetyl-CoA, MOF efficiently acetylated truncated human (h) TIP5 (Fig. 1c). Mass spectrometric analysis identified K649, a residue adjacent to the RNA binding domain, as a target of MOF-dependent acetylation (Supplementary Information, Fig. S2b). K649 in hTIP5 corresponds to K633 in mTIP5. *In vitro*, MOF acetylated K633, as monitored with a peptide-specific antibody raised against acetylated (ac) mTIP5 (Fig. 1d; Supplementary Information, Fig. S2c). *In vivo* overexpression of MOF enhanced acetylation of mTIP5, but not of the mTIP5<sup>K633R</sup> mutant. Acetylation

<sup>1</sup>German Cancer Research Center, Division of Molecular Biology of the Cell II, DKFZ-ZMBH Alliance, Im Neuenheimer Feld 581, D-69120 Heidelberg, Germany.

<sup>2</sup>European Molecular Biology Laboratory, Meyerhofstrasse 1, D-69117 Heidelberg, Germany.

<sup>3</sup>These authors contributed equally to this work.

<sup>4</sup>Correspondence should be addressed to: I.G. (e-mail: i.grummt@dkfz.de)

Received 4 March 2009; accepted 27 April 2009; published online 5 July 2009; DOI: 10.1038/ncb1914

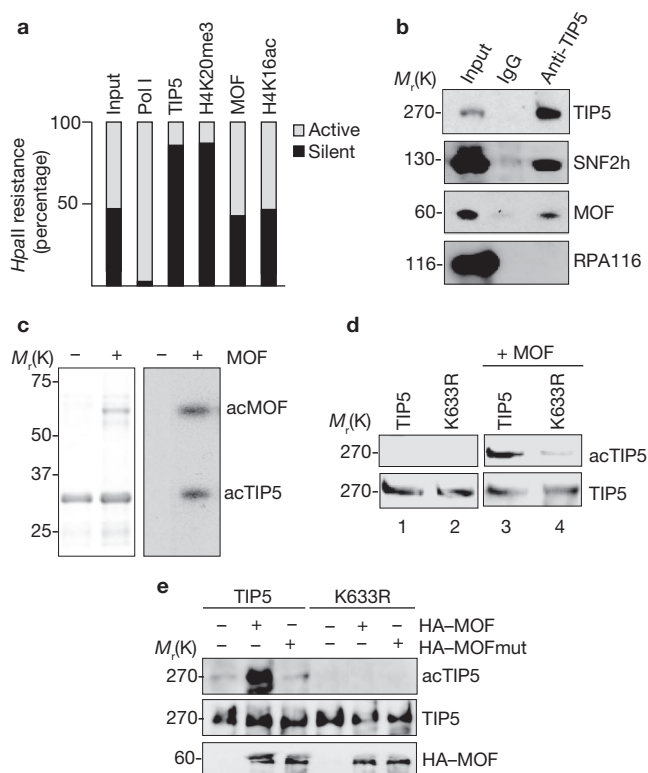


**Figure 1** MOF acetylates TIP5 *in vitro* and *in vivo*. **(a)** MOF is associated with active and silent rRNA genes. Crosslinked chromatin from NIH 3T3 cells was precipitated with the indicated antibodies, and precipitated DNA was either mock-digested or digested with *HpaII*. The relative levels of *HpaII*-resistant, inactive rDNA copies (dark bars) and unmethylated, active copies (light bars) were determined by qPCR using primer pair A that flanks the *HpaII* site (at -143) in mouse rDNA. **(b)** NoRC interacts with MOF *in vivo*. TIP5 was immunoprecipitated from nuclear extracts, and co-precipitated proteins were visualized on immunoblots using antibodies against SNF2h, MOF and Pol I (RPA116). **(c)** MOF acetylates human TIP5 *in vitro*. hTIP5<sup>510-723</sup> was incubated with MOF in the presence of [<sup>3</sup>H]-acetyl-CoA. Acetylation of TIP5 was detected by fluorography (right; acMOF, acetylated MOF; acTIP5, acetylated TIP5). The Coomassie-stained polyacrylamide gel is shown on the left. **(d)** MOF acetylates murine TIP5 at K633 *in vitro*. Flag- and HA-tagged mTIP5 and mTIP5<sup>K633R</sup> (K633R) were incubated with immunopurified MOF (lanes 3 and 4) in the presence of acetyl-CoA (10 μM). TIP5 was analysed on western blots with an anti-acK633-specific antibody (acTIP5) and an anti-Flag antibody (TIP5). **(e)** MOF acetylates mTIP5 *in vivo*. Flag-tagged mTIP5 and mTIP5<sup>K633R</sup> (K633R) were overexpressed in HEK293T cells in the absence and presence of HA-tagged wild-type MOF or mutant MOF<sup>G627D</sup> (HA-MOFmut). Acetylation of immunopurified TIP5 was assayed on western blots using an acK633-specific mTIP5 antibody (acTIP5). mTIP5 and MOF were monitored by immunostaining with anti-TIP5 (TIP5) and anti-HA antibodies (HA-MOF).

of mTIP5 did not occur in the presence of the HAT domain-deficient mutant MOF<sup>G627D</sup> (Fig. 1e).

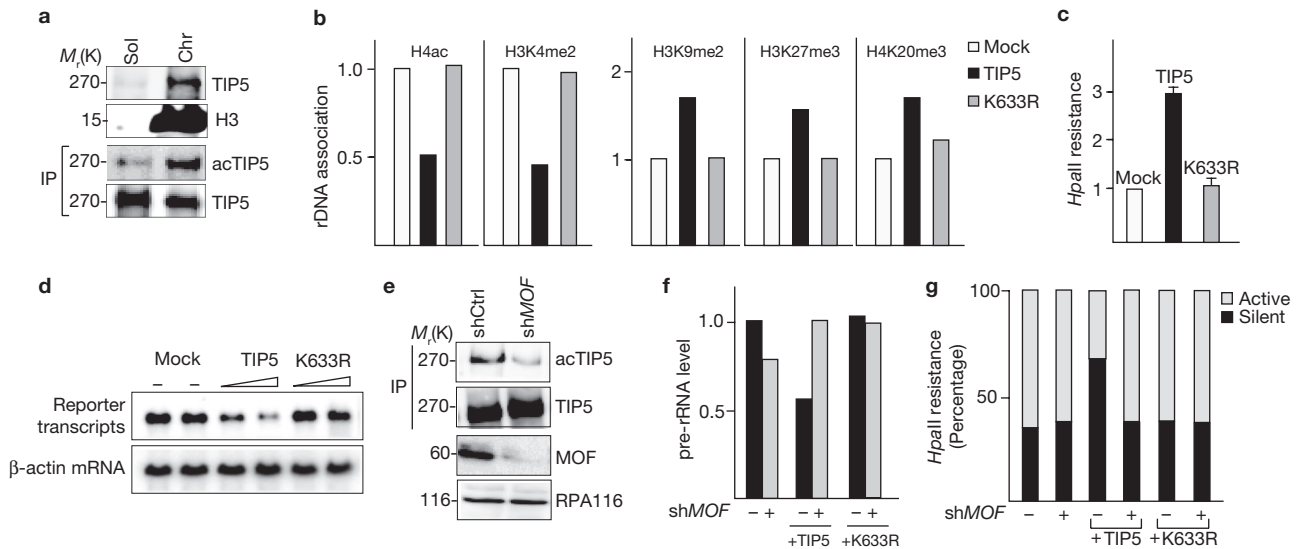
Cell fractionation experiments and quantitative western blots revealed that a minor fraction (7–11%) of cellular TIP5 was acetylated (data not shown) and that most of this acetylated TIP5 was associated with chromatin (Fig. 2a). Both mTIP5 and mTIP5<sup>K633</sup> localized to nucleoli and were tightly associated with chromatin, indicating that acetylation is not required for recruiting NoRC to rDNA (Supplementary Information, Fig. S3a–c). Overexpression of mTIP5 reduced euchromatic histone marks, such as H4ac and H3K4me2, and increased the level of repressive histone modifications, such as H3K9me2, H3K27me3 and H4K20me3

(Fig. 2b). In contrast, the acetylation-deficient mutant mTIP5<sup>K633R</sup> did not affect any of these histone modifications. In addition, mTIP5<sup>K633R</sup> was not capable of triggering *de novo* CpG (cytosine and guanine separated by a phosphate) methylation (Fig. 2c) or transcriptional repression of a co-transfected Pol I reporter plasmid (Fig. 2d), emphasizing the importance of K633 acetylation for heterochromatin formation and silencing. Consistently, short hairpin RNA (shRNA)-mediated knockdown of MOF led to hypoacetylation of TIP5 (Fig. 2e), abrogated transcriptional repression (Fig. 2f) and prevented NoRC-dependent *de novo* methylation of rDNA (Fig. 2g).

As NoRC function requires the association of TIP5 with pRNA (150–250 nucleotide RNAs that are complementary in sequence to the rDNA promoter)<sup>18,19</sup>, we examined the effect of TIP5 acetylation on pRNA binding. Contrary to our expectations, overexpression of MOF strongly decreased the level of pRNA associated with NoRC (Fig. 3a). Similarly, in pull-down experiments, acetylation by MOF strongly reduced the pRNA-binding activity of truncated mTIP5 (TIP5<sup>1-731</sup>), whereas three times more pRNA was associated with the acetylation-deficient mutant mTIP5<sup>K633</sup>, regardless of MOF coexpression (Fig. 3b). These results indicate that acetylation impairs the interaction of TIP5 with pRNA, an unexpected result given that pRNA binding is essential for NoRC function<sup>18</sup>. As NoRC is targeted to rDNA not only by binding to pRNA but also by interaction with TTF-I bound to its promoter-proximal target site T<sub>0</sub><sup>1</sup>, acetylation may also weaken the association of TIP5 with TTF-I. Indeed, co-immunoprecipitation experiments demonstrate enhanced interaction of TIP5<sup>K633R</sup> with TTF-I, supporting the notion that unacetylated NoRC is recruited to rDNA (Supplementary Information, Fig. S4).

To decipher the crosstalk between TIP5 acetylation, pRNA binding and NoRC function, we sought to artificially lower the affinity of mTIP5<sup>K633R</sup> for pRNA by introducing two point mutations (WY531,532GA) into its TAM domain. These two amino acid exchanges have been shown to impair the TIP5 interaction with pRNA and heterochromatin formation<sup>18</sup>. However, this mutant (mTIP5<sup>WY</sup>) was still capable of triggering DNA methylation and of silencing rDNA transcription. As expected, pRNA binding of mTIP5<sup>WYK633R</sup>, a mutant that is deficient in both RNA binding and K633 acetylation, was just as low as that of mTIP5<sup>WY</sup> (Fig. 3c; Supplementary Information, Fig. S5). Both mutants were less tightly associated with chromatin than wild-type TIP5, highlighting the importance of pRNA association for the binding of NoRC to chromatin (Supplementary Information, Fig. S3b). Surprisingly, mTIP5<sup>WYK633R</sup> efficiently triggered *de novo* DNA methylation and transcriptional silencing, implying that a weakened RNA binding enabled the acetylation-deficient mutant to function properly (Fig. 3d, e). The observation that impaired RNA binding rescues the silencing activity of mTIP5<sup>K633R</sup> demonstrates that both binding and release of pRNA are indispensable for NoRC function, and that reversible acetylation of TIP5 regulates its association and dissociation with pRNA.

Silencing of rRNA genes has been shown to require ATP-dependent nucleosome remodelling, which causes the promoter-bound nucleosome downstream of the transcription start site to shift into a translational position that is incompatible with transcription complex assembly<sup>13</sup>. To examine whether TIP5 acetylation is necessary for NoRC-dependent nucleosome repositioning, we digested crosslinked chromatin from cells overexpressing wild-type or mutant TIP5 with MNase and mapped the 5′-ends of mononucleosomal DNA by ligation mediated (LM)-PCR using linker- and rDNA-specific primers (Fig. 3f). Amplification of the reaction



products yielded two PCR fragments, the shorter one corresponding to promoter-bound nucleosomes at active genes (from -157 to -2) and the more slowly migrating one corresponding to nucleosomes at silent genes (from -132 to +22; ref. 13). In mock-treated cells, the ratio of the two PCR fragments was similar with ~60% of nucleosomes in the active and ~40% in the silent position. On overexpression of mTIP5, the levels of the two fragments changed to 20% and 80%, respectively, demonstrating that enhanced levels of NoRC increased the proportion of the downstream nucleosome position at the expense of the upstream one. Significantly, the RNA binding-deficient mutants mTIP5<sup>WY531,532</sup> and mTIP5<sup>WYK633R</sup>, but not the acetylation-deficient mutant TIP5<sup>K633R</sup>, were capable of shifting the nucleosome into the silent position. This result supports the notion that TIP5 acetylation promotes its dissociation from pRNA, a prerequisite for NoRC-dependent nucleosome positioning.

To identify the enzyme(s) that counteract *MOF*-dependent acetylation of K633, we monitored TIP5 acetylation after treating cells with specific deacetylase inhibitors. Trichostatin A (TSA) did not affect TIP5 acetylation, whereas inhibitors of NAD<sup>+</sup>-dependent deacetylases, including nicotinamide and splitomycin, enhanced K633 acetylation. Resveratrol, an activator of the NAD<sup>+</sup>-dependent deacetylase SIRT1, decreased K633 acetylation, suggesting that SIRT1 counteracts *MOF*-dependent acetylation of TIP5 (Fig. 4a). Consistently, overexpression of SIRT1, but not

the inactive mutant SIRT1<sup>H355Y</sup>, decreased K633 acetylation (Fig. 4b). In contrast, knockdown of SIRT1 enhanced K633 acetylation (Fig. 4c). Significantly, upon SIRT1 knockdown, TIP5 did not promote transcriptional repression and *de novo* DNA methylation (Fig. 4d, e), demonstrating the relevance of reversible acetylation for proper NoRC function.

Given that energy-dependent changes in the NAD<sup>+</sup>/NADH ratio regulates the activity of SIRT1, we examined NoRC acetylation and epigenetic changes at the rDNA promoter on glucose deprivation. Glucose depletion reduced pre-rRNA synthesis and decreased Pol I occupancy at the rDNA promoter (Fig. 4f, g). In addition, euchromatic histone marks, such as H4ac and H3K9ac, were decreased, whereas heterochromatic marks, such as H3K9me2 and H4K20me3, were increased (Fig. 4g). Elevated levels of heterochromatic histone modifications correlated with decreased binding of Pol I and enhanced binding of TIP5 to rDNA, in accord with a limited energy supply promoting NoRC-dependent heterochromatin formation (Fig. 4g). Consistent with glucose deprivation activating SIRT1 (refs 20, 21), the level of acetylated TIP5 dropped ~5-fold, whereas the amounts of SIRT1 and *MOF* were not altered (Fig. 4h). Significantly, deacetylation of TIP5 in glucose-depleted cells led to a significant increase in the level of NoRC-associated pRNA (Fig. 4i), again demonstrating the functional link between reversible TIP5 acetylation, pRNA binding and rDNA silencing.

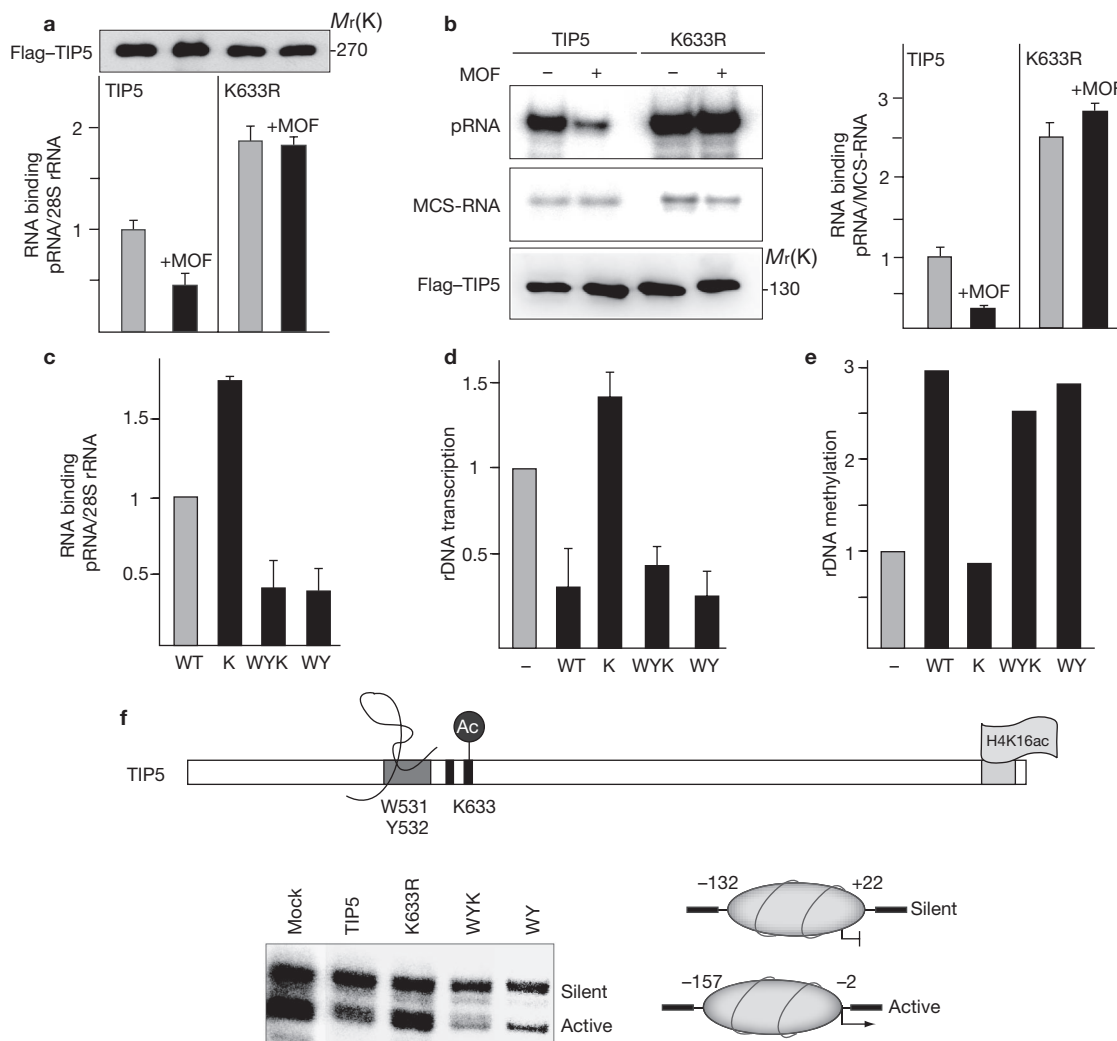


**Figure 3** Acetylation decreases pRNA binding to TIP5. **(a)** Acetylation alleviates the interaction of TIP5 with pRNA *in vivo*. Flag- and HA-tagged TIP5 and TIP5<sup>K633R</sup> were expressed in HEK293T cells in the presence or absence of GFP (green fluorescent protein)-tagged MOF. TIP5 was immunopurified and associated pRNA was analysed by RT-qPCR. Error bars indicate mean  $\pm$  s.d.,  $n = 3$ . The western blot shows immunoprecipitated TIP5. **(b)** The acetylation-deficient mutant TIP5<sup>K633R</sup> interacts most strongly with pRNA. Pull-down experiment using radiolabelled pRNA (upper left) or unspecific MCS-RNA (middle left) and immunopurified mTIP5<sup>1-731</sup> (TIP5) or mTIP5<sup>K633R1-731</sup> (K633R) overexpressed in HEK293T cells in the presence or absence of GFP-MOF. Bound RNA was analysed by electrophoresis and autoradiography. Bead-bound TIP5 was monitored on immunoblots (bottom left). The bar diagram (right) shows the level of bound pRNA normalized to MCS-RNA. Error bars indicate mean  $\pm$  s.d.  $n = 3$ . **(c)** *In vivo* RNA binding activity of mTIP5 (WT), mTIP5<sup>K633R</sup> (K), mTIP5<sup>WYK633R</sup> (WYK), and mTIP5<sup>WY531,532</sup> (WY). The respective HA- and Flag-tagged TIP5 proteins were immunoprecipitated and associated pRNA was analysed by RT-qPCR. Background levels without RT were subtracted. Error bars

indicate mean  $\pm$  s.d.,  $n = 3$ . **(d)** mTIP5<sup>WYK633R</sup> regains silencing activity. Transcriptional activity of NIH 3T3 cells harbouring a Pol I reporter plasmid (pMr131-BH) and expressing the TIP5 proteins specified in **c**. The bar diagram represents the level of reporter transcripts normalized to *GAPDH* mRNA. Error bars indicate mean  $\pm$  s.d.,  $n = 3$ . **(e)** mTIP5<sup>WYK633R</sup> induces *de novo* methylation of rDNA. Methylation of the reporter pMr131-BH in NIH 3T3 cells. Data represent the ratio of *Hpa*II-resistant to total rDNA, normalized to mock-transfected cells ( $n = 2$ ). **(f)** K633 acetylation is required for NoRC-dependent nucleosome positioning. Mononucleosomal DNA from mock-treated NIH 3T3 cells or cells expressing Flag-tagged mTIP5 (TIP5), mTIP5<sup>K633R</sup> (K633R), mTIP5<sup>WYK633R</sup> (WYK), or mTIP5<sup>WY531,532</sup> (WY) was subjected to LM-PCR. PCR products were separated on polyacrylamide gels (bottom left). The scheme at the top illustrates the domain structure of TIP5, the RNA-binding TAM domain (dark grey), AT-hooks (black) and the bromo domain (light grey) interacting with acetylated histone H4 (H4K16ac). Residues essential for RNA binding (W531, Y532) and acetylation (K633) are indicated. The scheme on the right depicts nucleosome positions at active and silent murine rDNA promoters.

If reversible acetylation regulates NoRC function, then changes in TIP5 acetylation should be most obvious during late S phase, that is, when the silent copies of rRNA genes are replicated and the heterochromatic state is inherited<sup>22</sup>. Indeed, the overall level of TIP5 was elevated in late S phase (5–6 h after release from G1/S), whereas TIP5 acetylation peaked earlier and declined to background levels in late S phase, consistent with a decrease in MOF and an increase in SIRT1 levels (Fig. 5a, b). TIP5, HDAC1 and

H4K20me3 occupancy on rDNA was also most pronounced 5 h after release from G1/S arrest (Fig. 5c). Importantly, the level of NoRC-associated pRNA was also elevated in late S phase, that is, when TIP5 acetylation was lowest (Fig. 5d). The inverse correlation between the acetylation state of NoRC and its association with pRNA and chromatin, reveals a mechanism by which reversible acetylation modulates NoRC binding to pRNA and propagates the heterochromatic state of silent rRNA genes through cell division.

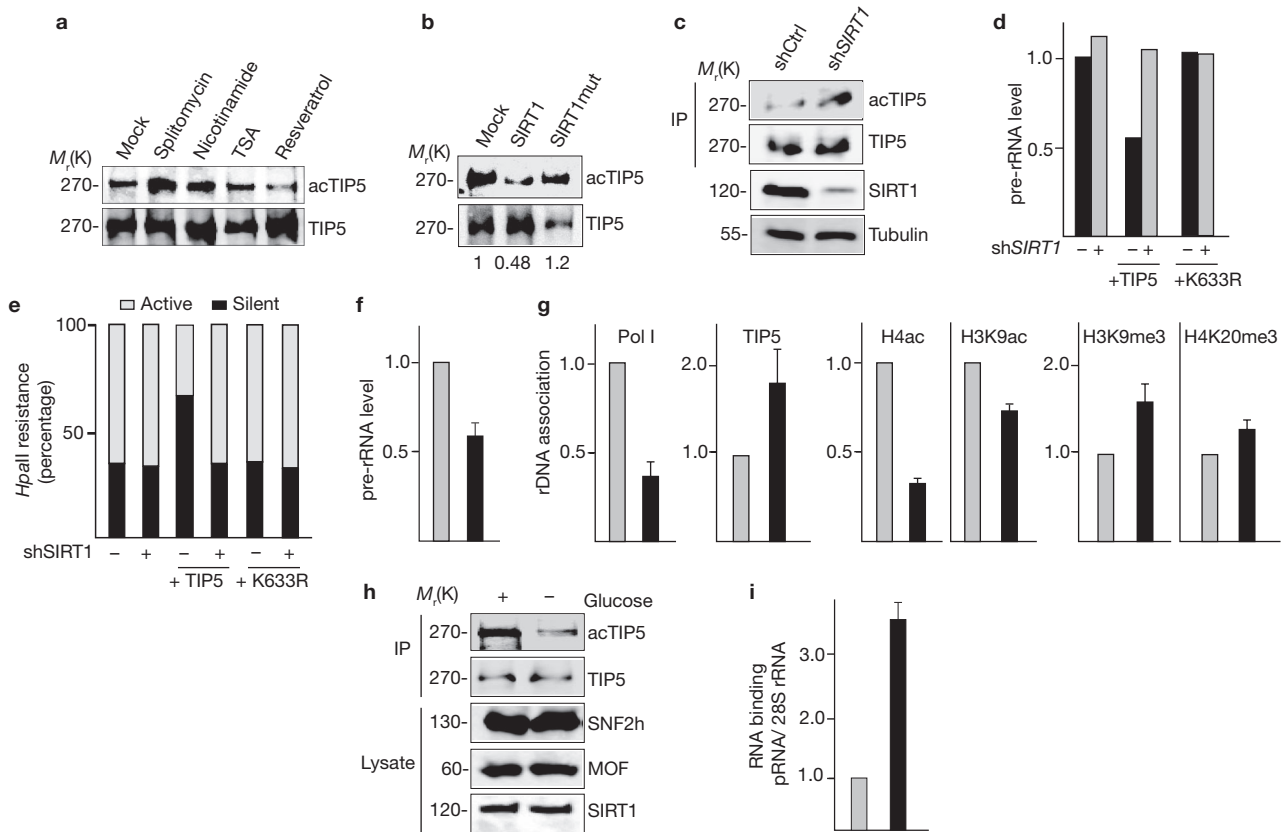


**Figure 4** Deacetylation by SIRT1 is required for NoRC function. **(a)** NAD<sup>+</sup>-dependent HDAC(s) deacetylate TIP5. HEK293T cells were treated for 16 h with splitomycin (120  $\mu$ M), nicotinamide (10 mM), TSA (33 nM) or resveratrol (5  $\mu$ M), and TIP5 was analysed on immunoblots using anti-TIP5 (TIP5) and anti-acK633 (acTIP5) antibodies. **(b)** SIRT1 deacetylates TIP5 *in vivo*. mTIP5 was immunoprecipitated from HEK293T cells co-expressing SIRT1 or SIRT1<sup>H355Y</sup> (SIRT1mut). TIP5 acetylation was assayed on immunoblots using anti-acK633 (acTIP5) and anti-TIP5 antibodies (TIP5). The numbers below the blots show the level of acTIP5 normalized to overall TIP5. **(c)** Knockdown of *SIRT1* decreases K633 acetylation. HEK293T cells expressing Flag and HA-tagged mTIP5 were treated with either control (shCtrl) or *SIRT1*-specific (shSIRT1) shRNA, and TIP5 levels were determined on immunoblots with anti-Flag (TIP5) and anti-acK633 antibodies (acTIP5; IP, immunoprecipitate). **(d)** Depletion of SIRT1 abolishes NoRC-mediated repression of pre-rRNA synthesis. NIH 3T3 cells expressing mTIP5 or mTIP5<sup>K633R</sup> were treated with control shRNA (-, dark bars) or *SIRT1*-specific shRNA (+, light bars) and pre-rRNA was analysed by

RT-qPCR. The bars represent pre-rRNA levels normalized to *GAPDH* mRNA from two experiments. **(e)** SIRT1 is required for NoRC-dependent *de novo* methylation of rDNA. NIH 3T3 cells specified in **d** were analysed for the level of *HpaII*-resistant, inactive rDNA copies (dark bars) and unmethylated active copies (light bars) by qPCR. Data are from two experiments. **(f)** Pre-rRNA synthesis is inhibited on glucose deprivation. RT-qPCR showing the levels of pre-rRNA in HEK293T cells cultured in glucose-rich (light bar) or glucose-deprived (dark bar) medium. Error bar indicates mean  $\pm$  s.d.,  $n = 3$ . **(g)** Glucose deprivation increases TIP5 binding and heterochromatic marks at rDNA. ChIP data from cells cultured in glucose-rich (light bars) or glucose-deprived (dark bars) medium. Error bars indicate mean  $\pm$  s.d.,  $n = 3$ . **(h)** Glucose deprivation leads to deacetylation of TIP5. TIP5, acTIP5, SNF2h, MOF and SIRT1 levels in HEK293T cells cultured in glucose-rich or glucose-deprived medium. **(i)** Glucose deprivation enhances binding of pRNA to NoRC. TIP5 was immunoprecipitated from cells grown in glucose-rich (light bar) and glucose-deprived (dark bar) medium and TIP5-associated pRNA was analysed by RT-qPCR. Error bar indicates  $\pm$  s.d.,  $n = 3$ .

The following model illustrates the role of acetylation and pRNA binding in NoRC-dependent heterochromatin formation and gene silencing (Fig. 5e). NoRC is recruited to rDNA by interaction with TTF-I bound to a target sequence upstream of the transcription start site<sup>1</sup> and by interaction with pRNA that matches the rDNA promoter<sup>18</sup>. Preliminary data indicate that binding to pRNA traps NoRC at the rDNA promoter. Therefore, transient dissociation of TTF-I and the release of pRNA is required for ATP-dependent chromatin remodelling and transcriptional silencing. Acetylation by MOF weakens the interaction between NoRC and both pRNA and TTF-I, and this change in RNA binding seems to be required for shifting the promoter-bound nucleosome downstream of the transcription start site into a translational position that is unfavourable for transcription complex formation<sup>13</sup>. In turn, NoRC-dependent re-positioning of the nucleosome at the rDNA promoter is required for DNA methylation by NoRC-associated DNA

methyltransferases (DNMTs). Methylation of a critical CpG residue within the upstream control element (UCE) has been shown to prevent binding of UBF to chromatin templates and to abrogate transcription complex formation<sup>23</sup>. To maintain and propagate the silent state of rDNA repeats through cell division, SIRT1 has to remove the acetyl group from K633 in late S phase. Deacetylation is required for re-association with pRNA, a prerequisite for heterochromatin formation and transcriptional silencing. Thus, acetylation by MOF and deacetylation by SIRT1 is instrumental for NoRC function. Together, our results reveal a crucial control mechanism that regulates epigenetic gene silencing by reversible acetylation of a chromatin remodelling complex, highlighting the close interrelationships between the acetyltransferase MOF, the NAD<sup>+</sup>-dependent deacetylase SIRT1 and the chromatin remodeller NoRC. The involvement of the NAD<sup>+</sup>-dependent deacetylase SIRT1 in the silencing process provides an opportunity to link

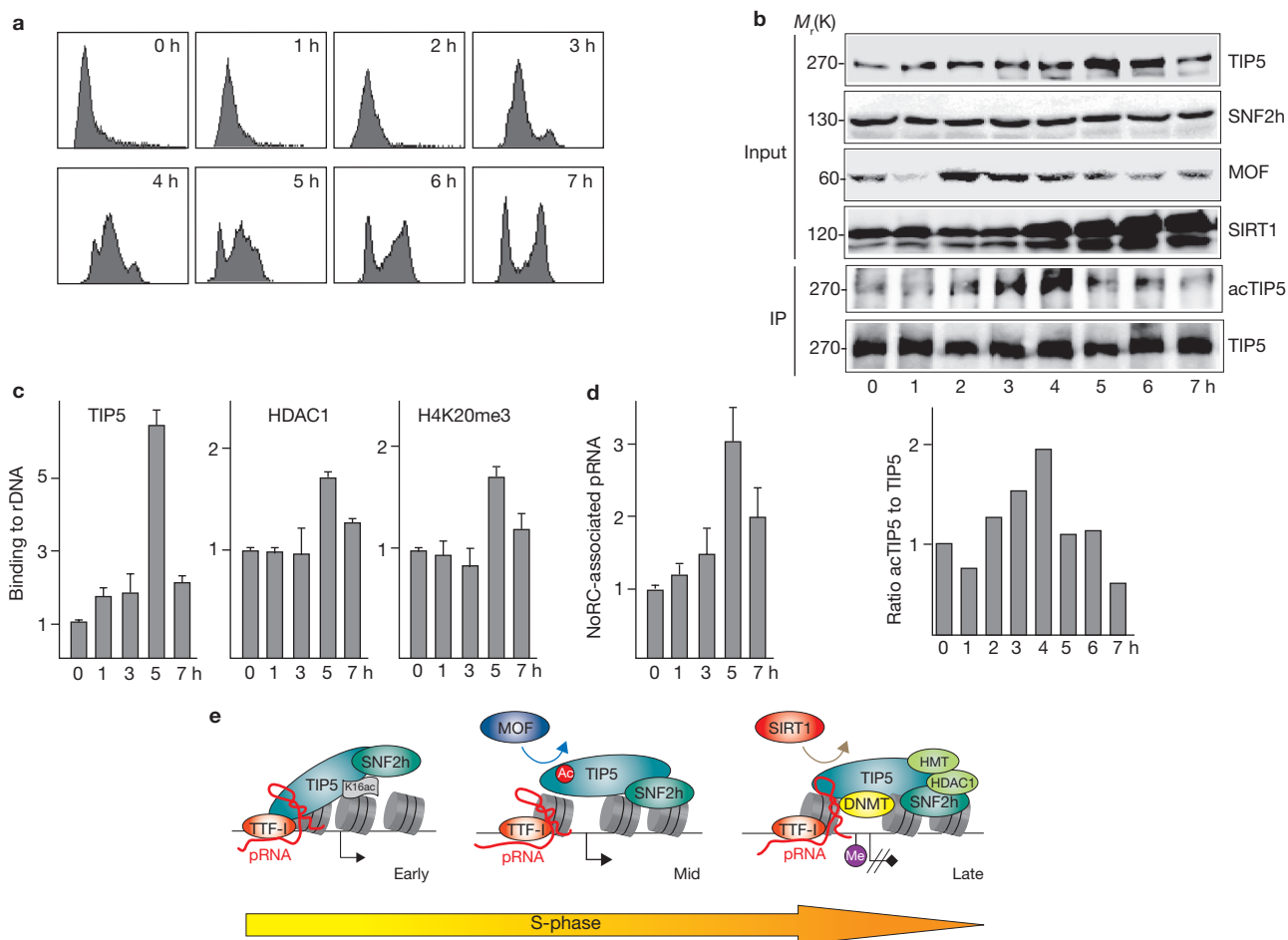


**Figure 5** Acetylation of TIP5 precedes replication of silent rDNA genes. **(a)** FACS demonstrating S-phase progression of synchronized L1210 cells. Cells were synchronized at G1/S by aphidicolin treatment and released into S phase by culturing in an aphidicolin-free medium. **(b)** Western blots showing the level of TIP5, SNF2h, MOF, SIRT1 and acetylated TIP5 (acTIP5) during S-phase progression. The upper blots show the amounts of the indicated proteins in lysates of arrested (0 h) and released (1–7 h) cells. TIP5 was immunoprecipitated at different times after release, and analysed on western blots (lower blots) with anti-TIP5 (TIP5) and anti-TIP5<sup>K633ac</sup> antibodies (acTIP5). The diagram (bottom) shows the quantification of acetylated TIP5 normalized to overall TIP5 levels during S phase. **(c)** ChIP data showing the association of TIP5, HDAC1 and H4K20me3 with the rDNA promoter during S phase. Error bars indicate mean  $\pm$  s.d.,  $n = 3$ . **(d)** RNA immunoprecipitation showing the association of pRNA with NoRC during S phase. Cells were synchronized as in **a**, TIP5 was immunoprecipitated at the indicated times after release from G1/S

and pRNA was analysed by RT-qPCR. The bar diagram shows the level of pRNA normalized to RNA from the coding region (+7,936/+8,036). Error bars indicate mean  $\pm$  s.d.,  $n = 3$ . **(e)** Model depicting the role of K633-acetylation in NoRC-dependent rDNA silencing. Distinct steps during S phase progression are illustrated. Early: TIP5 (turquoise) is recruited to rDNA by interactions with promoter-bound TTF-I, pRNA and H4K16ac. Mid: MOF acetylates chromatin-bound TIP5 at K633, leading to transient dissociation of pRNA and NoRC-dependent shifting of the promoter-bound nucleosome downstream of the transcription start site. Late: this nucleosome positioning allows *de novo* methylation by NoRC-associated DNMTs. Methylation of the promoter impairs UBF binding and pre-initiation complex assembly. To establish heterochromatic histone modifications and maintain the silent chromatin state, K633 has to be deacetylated by SIRT1, allowing re-association of NoRC with pRNA and the establishment of heterochromatic histone modifications (mediated by HMT and HDAC1) at the rDNA promoter.

cellular energy status to rDNA silencing, a process required for nucleolar integrity and cell survival<sup>24,25</sup>. □

Note: Supplementary Information is available on the Nature Cell Biology website.

## METHODS

Methods and any associated references are available in the online version of the paper at <http://www.nature.com/naturecellbiology/>.

## ACKNOWLEDGEMENTS

We thank S. Smale for providing the vector pQXCIP, L. Guarente for expression vectors encoding SIRT1<sup>H355Y</sup>, G. Xouri and M. Gentzel for their contribution at the early stages of this work and M. Wilm for his support in the mass spectroscopic analysis. This

study was funded by the Deutsche Forschungsgemeinschaft (SFB/Transregio 5, SP 'Epigenetics'), the EU-Network 'Epigenome' and the Fonds der Chemischen Industrie.

## AUTHOR CONTRIBUTIONS

Y.G., K.S., C.M. and I.G. conceived the experiments and wrote the manuscript. Y.G., K.S., C.M. and X.Y. performed and analysed the experiments and generated the figures. A.A. contributed the reagents and materials.

## COMPETING FINANCIAL INTERESTS

The authors declare no competing financial interests.

Published online at <http://www.nature.com/naturecellbiology/>.

Reprints and permissions information is available online at <http://npg.nature.com/reprintsandpermissions/>.

1. Strohner, R. *et al.* NoRC - a novel member of mammalian ISWI-containing chromatin remodeling machines. *EMBO J.* **20**, 4892–4900 (2001).
2. Zhou, Y., Santoro, R. & Grummt, I. The chromatin remodeling complex NoRC targets HDAC1 to the ribosomal gene promoter and represses RNA polymerase I transcription. *EMBO J.* **21**, 4632–4640 (2002).
3. Santoro, R., Li, J. & Grummt, I. The nucleolar remodeling complex NoRC mediates heterochromatin formation and silencing of ribosomal gene transcription. *Nature Genet.* **32**, 393–396 (2002).
4. Corona, D. F., Clapier, C. R., Becker, P. B. & Tamkun, J. W. Modulation of ISWI function by site-specific histone acetylation. *EMBO Rep.* **3**, 242–247 (2002).
5. Kurdistani, S. K., Tavazoie, S. & Grunstein, M. Mapping global histone acetylation patterns to gene expression. *Cell* **117**, 721–733 (2004).
6. Smith, E. R. *et al.* The *Drosophila* MSL complex acetylates histone H4 at lysine 16, a chromatin modification linked to dosage compensation. *Mol. Cell. Biol.* **20**, 312–318 (2000).
7. Akhtar, A. & Becker, P. B. Activation of transcription through histone H4 acetylation by MOF, an acetyltransferase essential for dosage compensation in *Drosophila*. *Mol. Cell* **5**, 367–375 (2000).
8. Lee, K. K. & Workman, J. L. Histone acetyltransferase complexes: one size doesn't fit all. *Nature Rev. Mol. Cell Biol.* **8**, 284–295 (2007).
9. Dou, Y. *et al.* Physical association and coordinate function of the H3 K4 methyltransferase MLL1 and the H4 K16 acetyltransferase MOF. *Cell* **121**, 873–885 (2005).
10. Hilfiker, A., Hilfiker-Kleiner, D., Pannuti, A. & Lucchesi, J. C. MOF, a putative acetyl transferase gene related to the *Tip60* and *MOZ* human genes and to the *SAS* genes of yeast, is required for dosage compensation in *Drosophila*. *EMBO J.* **16**, 2054–2060 (1997).
11. Buscaino, A. *et al.* MOF-regulated acetylation of MSL-3 in the *Drosophila* dosage compensation complex. *Mol. Cell* **11**, 1265–1277 (2003).
12. Zhou, Y. & Grummt, I. The PHD finger/bromodomain of NoRC interacts with acetylated histone H4K16 and is sufficient for rDNA silencing. *Curr. Biol.* **15**, 1434–1438 (2005).
13. Li, J., Längst, G. & Grummt, I. NoRC-dependent nucleosome positioning silences rRNA genes. *EMBO J.* **25**, 5735–5741 (2006).
14. Taipale, M. *et al.* MOF histone acetyltransferase is required for histone H4 lysine 16 acetylation in mammalian cells. *Mol. Cell. Biol.* **25**, 6798–6810 (2005).
15. Gupta, A. *et al.* Involvement of human MOF in ATM function. *Mol. Cell. Biol.* **25**, 5292–5305 (2005).
16. Smith, E. R. *et al.* A human protein complex homologous to the *Drosophila* MSL complex is responsible for the majority of histone H4 acetylation at lysine 16. *Mol. Cell. Biol.* **25**, 9175–9188 (2005).
17. Mendjan, S. *et al.* Nuclear pore components are involved in the transcriptional regulation of dosage compensation in *Drosophila*. *Mol. Cell* **21**, 811–823 (2006).
18. Mayer, C., Schmitz, K. M., Li, J., Grummt, I. & Santoro, R. Intergenic transcripts regulate the epigenetic state of rRNA genes. *Mol. Cell* **22**, 351–361 (2006).
19. Mayer, C., Neubert, M. & Grummt, I. The structure of NoRC-associated RNA is critical for targeting the chromatin remodeling complex NoRC to the nucleolus. *EMBO Rep.* **9**, 774–778 (2008).
20. Rodgers, J. T. *et al.* Nutrient control of glucose homeostasis through a complex of PGC-1 $\alpha$  and SIRT1. *Nature* **434**, 113–118 (2005).
21. Fulco, M. *et al.* Glucose restriction inhibits skeletal myoblast differentiation by activating SIRT1 through AMPK-mediated regulation of Nampt. *Dev. Cell* **14**, 661–673 (2008).
22. Li, J., Santoro, R., Koberna, K. & Grummt, I. The chromatin remodeling complex NoRC controls replication timing of rRNA genes. *EMBO J.* **24**, 120–127 (2004).
23. Santoro, R. & Grummt, I. Molecular mechanisms mediating methylation-dependent silencing of ribosomal gene transcription. *Mol. Cell* **8**, 719–725 (2001).
24. Murayama, A. *et al.* Epigenetic control of rDNA loci in response to intracellular energy status. *Cell* **133**, 627–639 (2008).
25. Grummt, I. & Ladurner, A. G. A metabolic throttle regulates the epigenetic state of rDNA. *Cell* **133**, 577–580 (2008).

## METHODS

**Plasmids, cell lines and cell synchronization.** Expression vectors encoding TIP5 and truncation mutants of TIP5 (refs 1, 13), MOF (ref. 14), SIRT1 (ref. 26) and the reporter plasmid pMr131-BH<sup>12</sup> have been described previously. The RNA binding-deficient mutant TIP5<sup>WY531,532</sup> contains two amino acid exchanges within the TAM domain<sup>18</sup>. To generate the acetylation-deficient mutant TIP5<sup>K633R</sup>, K633 was replaced by arginine. Mutant TIP5<sup>WYK633R</sup> is a fusion of TIP5<sup>WY531,532</sup> and TIP5<sup>K633R</sup>. shRNA against MOF (5'-gtgatcagctctcgatga-3') and SIRT1 (5'-gatgaagttgacctctca-3') was cloned into the retroviral vector pQXCIP<sup>27</sup>. Mouse L1210 cells were synchronized at G1/S by aphidicolin (2 µg ml<sup>-1</sup> for 12 h), released into aphidicolin-free medium for 10 h, and then cultured for another 14 h in the presence of aphidicolin. For glucose deprivation, cells grown in DMEM (with 25 mM glucose) were washed twice with PBS and cultured in glucose-free medium for 24 h.

**Chromatin immunoprecipitation (ChIP) and DNA methylation assays.** Crosslinked chromatin was incubated with antibodies and immunoprecipitated proteins were bound to protein A/G Sepharose. After reversal of the crosslink and digestion with proteinase K, DNA was extracted and amplified using quantitative (q)PCR. The ratio of rDNA in the immunoprecipitates versus rDNA in the input chromatin was normalized to that from control reactions in mock-treated cells. Data from ChIP assays using antibodies for specific histone modifications were normalized to data from histone H3 ChIP assays. To monitor CpG methylation, DNA was digested with *HpaII* (20 U per µg DNA) before PCR amplification. The relative resistance to *HpaII* digestion was normalized to mock- and *MspI*-digested DNA<sup>23</sup>. Primers used to amplify human or mouse rDNA have been described previously<sup>28</sup>.

**Transfection and RNA analysis.** Mouse NIH 3T3 cells (3 × 10<sup>5</sup>) were transfected with the Pol I reporter plasmid pMr131-BH (1 µg) and different amounts of expression vectors encoding wild-type or mutant Flag- or HA-tagged TIP5. For stable expression of TIP5, NIH 3T3 cells were infected with a retrovirus encoding wild-type or mutant mTIP5 and cultured for 4–5 days in the presence of puromycin (5 µg ml<sup>-1</sup>) before collection. Transcripts from the reporter plasmid were monitored on northern blots by hybridization to a <sup>32</sup>P-labelled riboprobe that is complementary to pUC9 sequences inserted between the 5'- and 3'-terminal rDNA fragment in pMr131-BH. Alternatively, transcripts were analysed by RT-qPCR and normalized to *GAPDH* mRNA.

**Purification of recombinant proteins and cell fractionation.** For acetylation assays, histidine-tagged hTIP5 was expressed in *Escherichia coli* BL21(DE3) cells and purified on Ni-NTA agarose (Qiagen). For functional studies, TIP5 was immunopurified from human HEK293T cells overexpressing Flag- and HA-tagged TIP5. To assay the association of NoRC with chromatin, nuclei were extracted twice with 10 mM Pipes at pH 7.0, 420 mM NaCl, 3 mM MgCl<sub>2</sub>, 0.2 mM EDTA and 0.5 mM dithiothreitol, and lysed; chromatin was dissolved in 10 mM Pipes at pH 7.0, 420 mM NaCl, 10 mM MgCl<sub>2</sub> and 0.5% Triton X-100. After sonication, chromatin was incubated with benzonase (for 30 min, 30 U), cleared by centrifugation and immunoblotted to determine the distribution of TIP5 in the chromatin-bound and soluble fractions.

**RNA binding assays and RNA immunoprecipitation (RIP).** HEK293T cells overexpressing Flag- and HA-tagged truncated TIP5<sup>1-731</sup> were lysed in 500 µl of L-buffer (20 mM Tris-HCl at pH 7.4, 200 mM NaCl, 2 mM EDTA, 2 mM EGTA, 1% Triton X-100, 3.5 mM sodium butyrate, 5 ng ml<sup>-1</sup> TSA and 10 mM nicotinamide) and incubated for 3 h with M2-agarose beads. Bead-bound TIP5 was incubated for 30 min on ice with *in vitro* transcribed radiolabelled pRNA or non-specific RNA derived from the multiple cloning site (MCS-RNA) of pBluescript-KS/*EcoRI*<sup>18</sup>. Beads were washed successively in buffer A (20 mM Tris-HCl at pH 7.6, 5 mM MgCl<sub>2</sub> and 0.2 mM EDTA) containing 200 mM KCl, 400 mM KCl

or 600 mM KCl. Retained proteins were quantified by liquid scintillation counting or analysed on 8% denaturing polyacrylamide gels. For RIP experiments, lysates from HEK293T cells were incubated with M2-agarose beads for 3–5 h. Beads were washed twice, first with a buffer containing 400 mM NaCl and then with a buffer containing 200 mM NaCl. pRNA and control RNAs (*β-actin*, *GAPDH* and 28S rRNA) levels were quantified by RT-qPCR; reactions without reverse transcriptase served as negative controls<sup>13</sup>.

**Analysis of nucleosome positions by LM-PCR.** Analysis of nucleosome positions at the rDNA promoter has been described previously<sup>13</sup>. Briefly, cells were crosslinked with 1% formaldehyde and permeabilized with 0.05% lysolecithin for 1 min. DNA was digested with MNase (15 U ml<sup>-1</sup>; Roche) in 150 mM sucrose, 50 mM Tris-HCl at pH 7.4, 50 mM NaCl and 2 mM CaCl<sub>2</sub> for 30 min at room temperature. After reversal of crosslinking, mononucleosome-sized DNA was isolated from 2% agarose gels and ligated to linker oligonucleotides (linker S: 5'-gaattcagatc-3' and linker L: 5'-gcggtgaccggagatctgaattc-3') phosphorylated with T4 polynucleotide kinase. Purified DNA was amplified by PCR using a linker primer and a 5'-labelled rDNA-specific primer (-105/-87). PCR products were separated on 8% polyacrylamide gels and analysed by autoradiography.

**In vitro acetylation by MOF.** Acetylation reactions contained 0.2 µg HA-MOF, 1 µg hTIP5<sup>510-732</sup> and 0.05 µCi [<sup>3</sup>H]-labelled acetyl-CoA in 20 mM Tris-HCl at pH 8.8, 1.5 mM MgCl<sub>2</sub> and 20 mM NaCl. After incubation for 1 h at 30°C, proteins were separated by 15% SDS-PAGE and analysed by fluorography. For mass spectrometric analysis of TIP5 acetylation, the assays were performed in the presence of unlabelled acetyl-CoA (10 µM).

**Knockdown of MOF and SIRT1.** Cells (6 × 10<sup>5</sup>) were transfected twice with 100 pmol of short interfering RNA (siRNA) against *MOF* (5'-gugaucagucgaguga-3')<sup>14</sup> using the TransIT-TKO transfection Reagent (Mirus). Cells were collected 3 days after the first knockdown. NIH 3T3 cells were infected with a retrovirus encoding shRNA against *MOF* or *SIRT1* and collected after 5 days.

**Antibodies.** Antibodies against TIP5 (ref. 1) and MOF<sup>14</sup> have been described previously. To generate antibodies that specifically recognize mTIP5 acetylated at K633 (anti-mTIP5<sup>K633ac</sup>), rabbits were immunized with an acetylated mTIP5 peptide (PPKlAcKMPELC, acK representing acetylated K633). Commercial antibodies were purchased from the following companies: anti-Flag (M2) antibody from Sigma, anti-H4K20me3, anti-HDAC1 and anti-HA antibodies from Abcam, and antibodies against SIRT1, acetylated histone H4 (H4ac), H4K16ac, H3K4me2, H3K9me2 and H3K27me3 from Upstate Biotechnology.

**Statistical analysis.** Error bars denote mean ± s.d. from three to four independent experiments.

**Mass spectrometry.** Bands were excised from the gel and proteins were digested with trypsin according to standard protocols. Extracted peptides were separated by Nano-HPLC with a linear gradient of water/acetonitrile/formic acid at a flow rate of 60 nl min<sup>-1</sup> on a reversed phase column. Lysine-acetylated peptides were detected by precursor-ion-like scanning. Acetylated amino acids were verified by subsequent peptide sequencing using HPLC-MS/MS.

26. Frye, R. A. Characterization of five human cDNAs with homology to the yeast *SIR2* gene: Sir2-like proteins (sirtuins) metabolize NAD and may have protein ADP-ribosyltransferase activity. *Biochem. Biophys. Res. Commun.* **260**, 273–279 (1999).
27. Ramirez-Carrozzi, V. R. *et al.* Selective and antagonistic functions of SWI/SNF and Mi-2 $\beta$  nucleosome remodeling complexes during an inflammatory response. *Genes Dev.* **20**, 282–296 (2006).
28. Schmitz, K. M. *et al.* TAF12 recruits Gadd45a and the nucleotide excision repair complex to the promoter of rRNA genes leading to active DNA demethylation. *Mol Cell* **33**, 344–353 (2009).

DOI: 10.1038/ncb1914

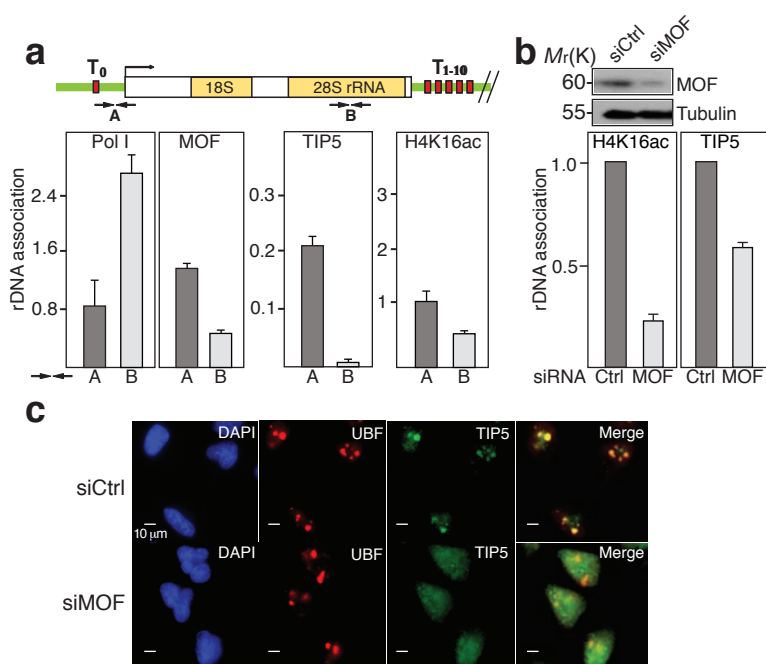


**Figure S1** Depletion of MOF impairs NoRC association with rDNA. MOF is associated with rDNA. ChIP data showing the association of Pol I, MOF, TIP5 and H4K16ac with the respective regions of rDNA normalized to input DNA. Data are the average from two independent experiments. The scheme above shows the organization of a murine rDNA transcription unit and the position of the PCR primers, highlighting the position of the upstream terminator  $T_0$  and the downstream terminators  $T_1$ - $T_{10}$ . The transcription start

site is marked by an arrow. **(b)** Knockdown of MOF impairs NoRC binding to chromatin. ChIP showing rDNA promoter occupancy of H4K16ac and mTIP5 in HeLa cells treated with control (dark bars) and MOF-specific siRNA (light bars). The western blot above shows the knockdown of MOF. **(c)** Depletion of MOF by siRNA releases NoRC from nucleoli. HeLa cells were treated with either control siRNA (siCtrl) or MOF-specific siRNA (siMOF), and localization of NoRC (TIP5) and UBF was visualized by indirect immunofluorescence.

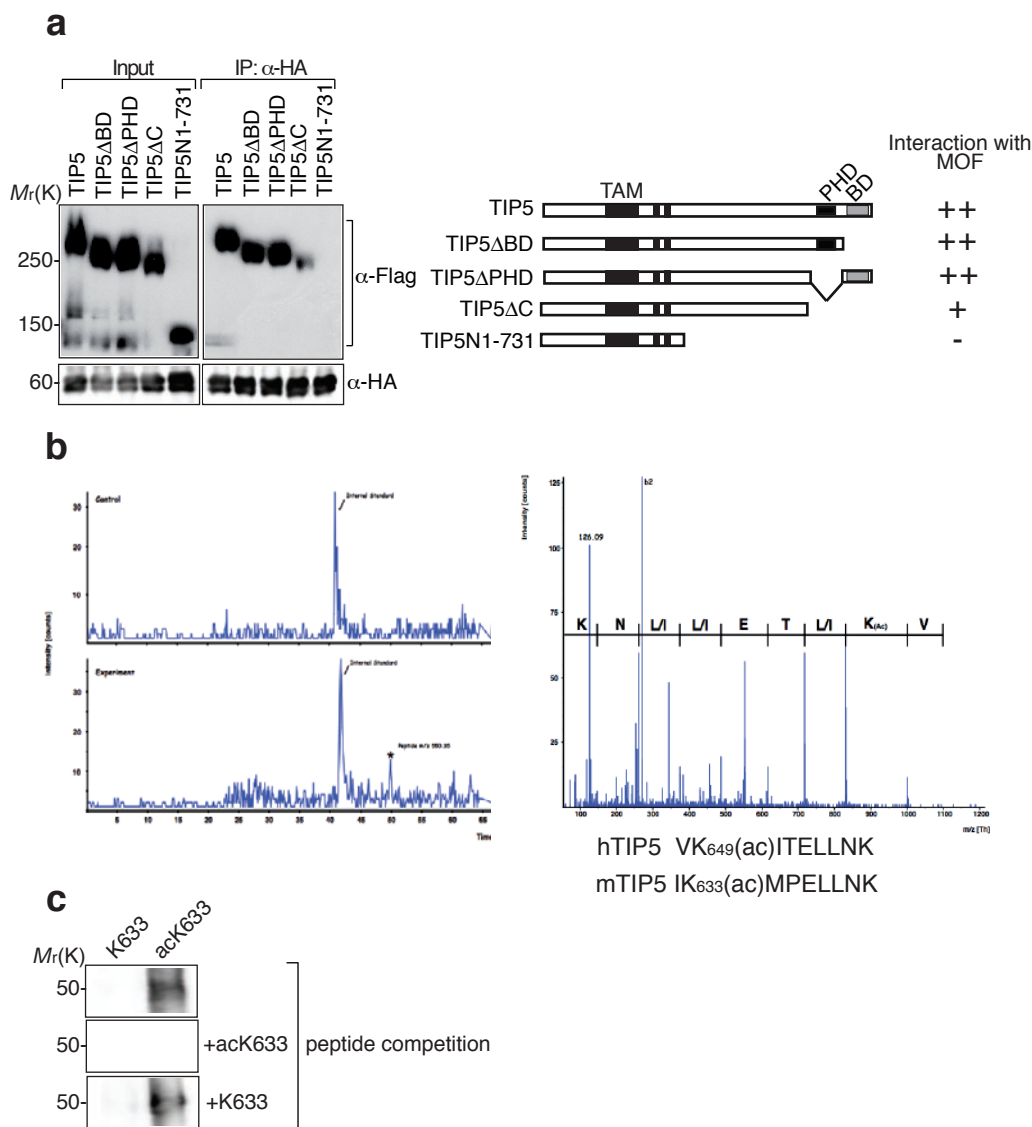


**Figure S2** MOF interacts with and acetylates mTIP5. The central part of TIP5 interacts with MOF *in vitro*. Left panel: Flag-tagged TIP5 and the indicated deletion mutants were co-expressed with HA-tagged MOF in HEK293T cells. MOF was precipitated and coprecipitated TIP5 derivatives were analyzed on immunoblots. Right panel: The scheme shows mTIP5, the C-terminal deletions and a summary of the interaction data. The positions of the TAM domain, the PHD finger and the bromodomain (BD) are indicated. Mass spectrometric analysis of *in vitro* acetylated hTIP5.

hTIP5<sub>510-723</sub> was acetylated by MOF in the presence of acetyl-CoA and subjected to mass spectrometry. A sequence alignment of the tryptic peptides that are acetylated in hTIP5 (at K649) and mTIP5 (at K633) is shown below. Western blot showing that anti-mTIP5acK633 antibody specifically recognizes ovalbumine coupled acetylated TIP5 peptide. Immunoblots with anti-mTIP5acK633 antibodies were performed in the presence of the acetylated (acK633) peptide that was used for immunization (PPKIKacMPELLC) or in the presence of the unacetylated peptide (K633).

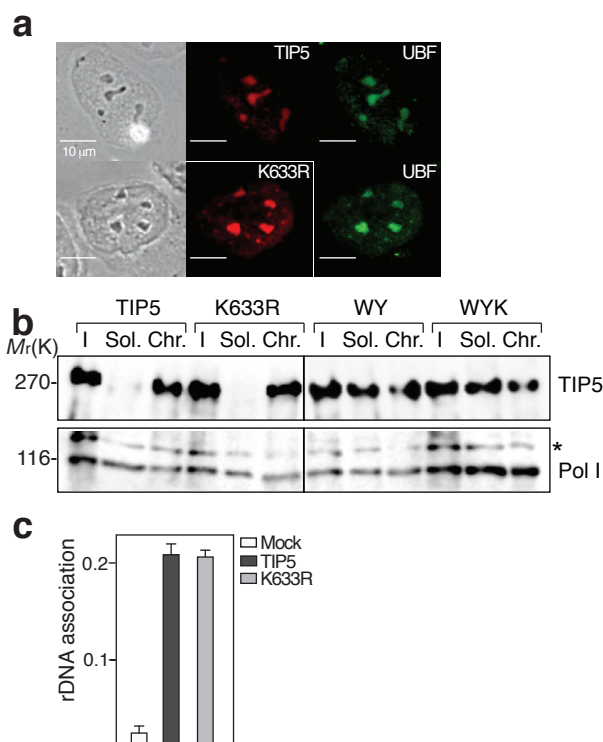


**Figure S3** Chromatin association and cellular localization of wildtype and mutant TIP5. mTIP5 and mTIP5K633R localize in nucleoli. Phase contrast images and immunostainings of UBF and TIP5 in U2OS cells overexpressing Flag-tagged wildtype or mutant mTIP5<sub>1-732</sub> are shown. **(b)** Acetylation does not alter the association of mTIP5 with chromatin. Nuclei from HEK293T cells expressing Flag/HA-tagged mTIP5, mTIP5K633R (K), mTIP5WY531/532 (WY) or mTIP5WYK633R

(WYK) were either lysed (I) or fractionated into chromatin (Chr) and nucleoplasm (Sol). TIP5 and Pol I levels were monitored on immunoblots with anti-Flag (TIP5) and anti-RPA116 antibodies. **(c)** TIP5 acetylation does not affect the association of NoRC with rDNA. The bars represent the results from ChIP assays showing the association of mTIP5 and mTIP5K633R with the rDNA promoter (% of input). Error bars indicate +/- SD (n=3).

## SUPPLEMENTARY INFORMATION

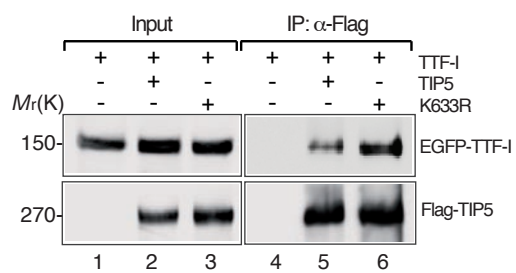


**Figure S4** TIP5K633R interacts more efficiently with TTF-I. HEK293T cells were transfected with expression vectors encoding GFP-tagged TTF-I and Flag/HA-tagged TIP5 or TIP5K633R as indicated. TIP5 was precipitated with anti-Flag antibody and co-precipitated TTF-I was monitored on immunoblots using anti-GFP antibodies.

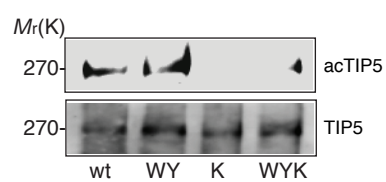


**Figure S5** Mutation of WY531/532 in the TAM domain does not alter K633 acetylation of TIP5. Flag/HA-tagged mTIP5, mTIP5WY531/532, mTIP5K633R, and mTIP5WYK633 (TIP5, WY, K, WYK, respectively) were

immunopurified from HEK293T cells and the levels of acetylation of TIP5 were monitored on immunoblots with anti-Flag (TIP5) and anti-acK633 antibodies (acTIP5).

SUPPLEMENTARY INFORMATION

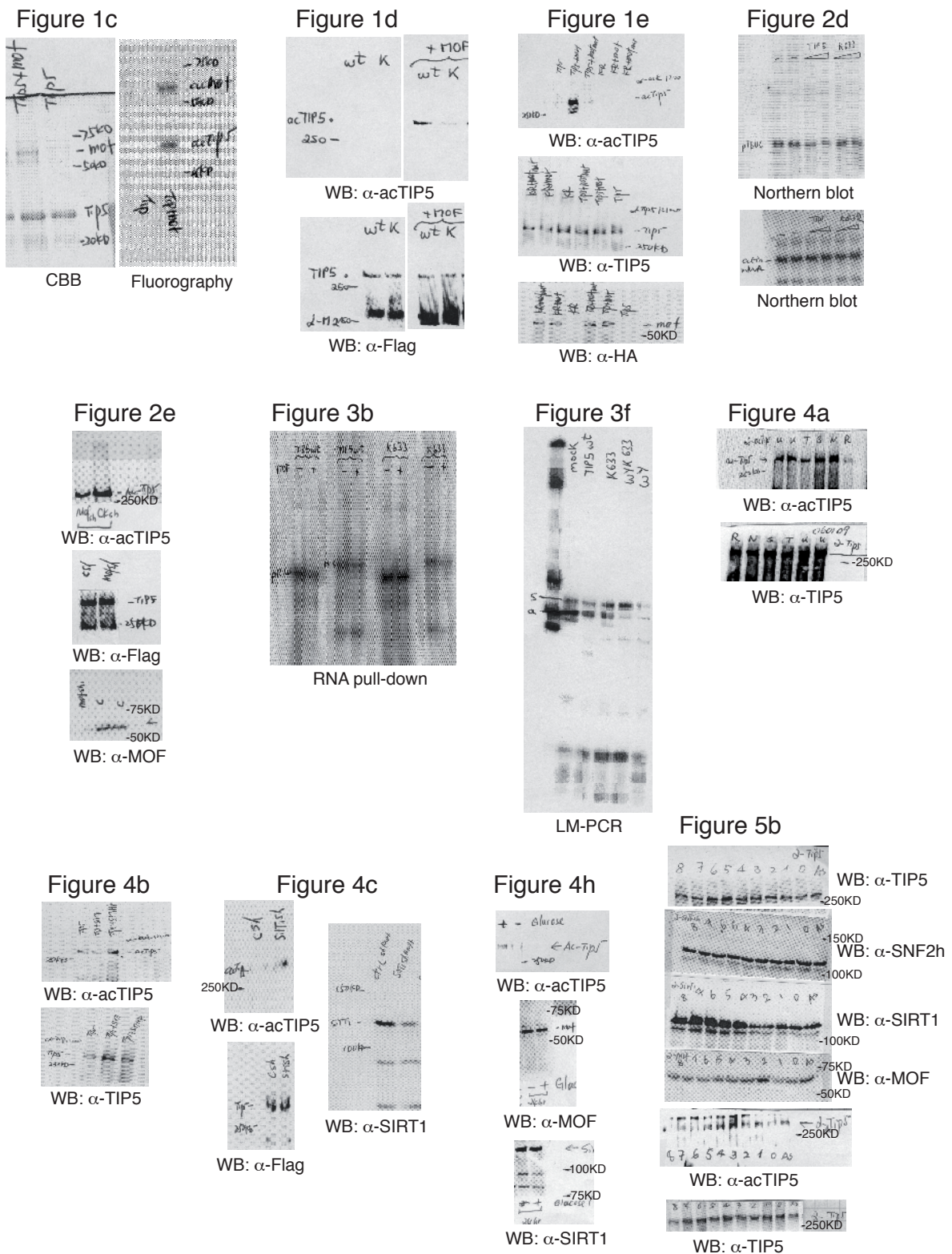


Figure S6 Original scans of selected autoradiograms and western blots.